Novel glass-ceramic composition as sealant for SOFCs

F. Smeacetto [a*], A. De Miranda [a], A. Chrysanthou [b], E. Bernardo [c] , M. Secco [d], M. Bindi [e], M. Salvo [a] , A. G. Sabato [a] and M. Ferraris [a]

[a] *Department of Applied Science and Technology, Politecnico di Torino, Corso Duca degli Abruzzi 24, 10129, Torino, Italy*

[b] *School of Engineering and Technology, University of Hertfordshire, Hatfield, Herts AL10 9AB*

[c] *Department of Industrial Engineering, Universita' degli Studi di Padova, Via Marzolo, 9 35131 Padova, Italy*

[d] *Department of Geosciences, Universita' degli Studi di Padova, Via Gradenigo, 6 35131 Padova, Italy*

[e] *Edison Research & Development Center, Edison S.p.A., Trofarello, Torino, Italy*

[*] *Corresponding author: Dr. Federico Smeacetto, e-mail: federico.smeacetto@polito.it*
Tel+390110904756; fax +390110904699

Keywords: solid oxide fuel cell, microstructure, sealant, glass-ceramic

Abstract

This work deals with the design, the characterization and testing of a novel glass-ceramic to be used as sealant for planar solid oxide fuel cells and its compatibility with $Mn_{1.5}Co_{1.5}O_4$ coated Crofer22APU. Thermal, sintering and crystallization behaviour and thermo mechanical properties of the sealant are reviewed and discussed, indicating therefore that these compositions can be deposited at 850°C and provide an excellent compatibility with both the $Mn_{1.5}Co_{1.5}O_4$ coated Crofer22APU and the anode supported electrolyte. In particular, $Mn_{1.5}Co_{1.5}O_4$ coated Crofer22APU/sealant/anode-supported-electrolyte joined samples have been submitted to thermal tests (in air atmosphere) from RT to 800°C (SOFC operating temperature) up to 500 hrs. No

interactions, cracks formation or failure were observed at the $Mn_{1.5}Co_{1.5}O_4$ coated Crofer22APU/sealant interface and between the glass-ceramic and the anode-supported-electrolyte after 500 hours of thermal tests in air atmosphere.

1. Introduction

Owing to their design, planar solid oxide fuels cells (SOFC) offer higher power density in comparison to tubular SOFC [1]. However, the planar stack designs require seals to prevent the mixing of fuel and oxidant gases. A significant challenge in SOFC technology is presented by the development of sealant materials [2, 3], since they must meet very critical and restrictive requirements. Sealants must withstand the severe environment of the SOFC (both oxidative and reducing environment) and be thermo mechanically and chemically compatible with the cell and the interconnect materials. In particular, a critical issue in the fabrication of planar SOFCs is the sealing of the electrolyte (supported on the anode) with the metallic interconnect [4, 5]. One of the major technological difficulties for commercialisation of SOFCs is the need to meet these requirements and be cost-effective and maintain reliable performance. Among the candidate materials, glasses and glass-ceramics are likely to be the materials of preference as they exhibit better resistance to the severe service environment (oxidizing and reducing) than brazing alloys [6-14]. The problem of materials choice becomes even more challenging as there is also a requirement for thermal cycle stability for planar stacks in which different SOFC components with dissimilar thermo-mechanical properties are joined together. The sealants must endure high operating temperatures for many thermal cycles from room temperature to the SOFC operating temperature of 750°C to 800°C. The mismatch in the coefficient of thermal expansion (CTE) between the sealant and the anode, the electrolyte and the cathode together with the intrinsic brittleness of glasses are the critical factors that may determine whether cracks develop in the sealants during thermal cycling. This can cause gas leakage that would lower the cell efficiency and performance. In order to maintain a gas tight seal, the sealant must exhibit strong bonding

with the materials to which is in contact. In addition, interfacial reactions must not lead to products with thermal expansion different from those of the original phases, otherwise high residual stresses will be generated within the interfacial reaction area giving rise to cracks and consequently to path for gases. In addition, the formation of any physically and chemically unstable products must be avoided.

Glasses can be deposited on metal and ceramic substrates in the form of slurries or pastes (dispersions of glass powders in organic vehicles with different solid to liquid ratio). Heat treatment at temperatures above the glass softening points are required to allow a good wetting of the substrates by means of viscous flow sintering. A large number of glass systems are described in the literature as being suitable for joining ceramic cells and metallic interconnects (Cr containing stainless steels) and act as sealants in planar SOFCs.

The glass-ceramic composition that is presented here was selected and chosen according to the following issues: alkali contribute to decrease characteristic temperatures, to adjust glass viscosity, to improve the wettability of glasses and to provide CTE matching. This composition was chosen for its excellent sintering and densification behavior at a deposition temperature of 850°C. Recently, in literature some groups reported on alkali alumino-silicate glasses [ref 6, 10 and 12]; in particular Y.-S. Chou, E.C. Thomsen, J.P. Choi, J.W. Stevenson, J. Power Sources 197 (2012) 154-160 and Y.-S. Chou, E.C. Thomsen, R.T. Williams, J.P. Choi, N.L. Canfield, J.F. Bonnett, J.W. Stevenson, A. Shyam, E. Lara-Curzio, J. Power Sources 196 (2011) 2709-2716, reported the compatibility between Crofer22APU and potassium oxide containing glasses, but without presenting discussion about corrosion mechanism, like alkali chromates formation and their volatility.

In our previous earlier works [see ref 8, 14 and 18] we presented alkali containing glass-based sealant; for that particular composition the Na and Ca diffused away from the interface and also

for 3000 hrs, and also no weight change was observed after the thermal tests. Moreover, we did not observe detrimental reaction at the interface and no cathode poisoning.

Glass systems proposed in the literature have sealing temperatures ranging from 780°C to 950°C, depending on their composition and thermal properties. However, there are two main problems associated with the use of chromia-forming alloy interconnects in SOFC devices; evaporation and migration of Cr from the chromia scale and the electrical resistance increase over time due to continuous oxidation at high temperatures.

Previous investigations [15-17] have suggested that Mn–Co oxides are the most promising coating materials for protecting the steel interconnect and improving SOFC performance. (Mn,Co)3O4 spinel is one of the most promising coatings due to its high electrical conductivity, good CTE match with the metallic interconnect and a very good chromium retention capability. The compatibility of Mn–Co oxide coatings with glass-based sealants has been studied by various researchers [18–20] showing prevention of Cr diffusion and prevention of any chemical interaction between the sealant and the coating.

In order to be hermetic, the Mn-Co oxide coated interconnect /sealant interface should be pore- and crack-free and exhibit stability during the cell operation. Accordingly, requirements such as high adhesion and bond strength between the glass and the coated interconnect as well as minimal interdiffusion and no chemical reaction.

The current study aimed to investigate the thermo-mechanical properties and the sintering behaviour of a new sealant formulation and to examine the medium-term (500 hrs) thermal behaviour of $Mn_{1.5}Co_{1.5}O_4$-coated Crofer22APU-sealant-anode supported electrolyte joints, with particular focus on the $Mn_{1.5}Co_{1.5}O_4$-coated Crofer22APU/sealant interfacial stability. The proposed system has the advantage to have an excellent sintering and densification behaviour at a deposition temperature of 850°C.

2. Experimental

The anode-supported electrolyte (ASE) (electrolyte: 8%mol yttria stabilized cubic zirconia, YSZ; anode; NiO-YSZ) half-cell was purchased from H. C. Starck GmbH (Germany). The Crofer22APU (Tyssen Krupp, Germany) and ASE samples to be joined were cut to obtain a final joined sample of 5 × 5× 2 mm^3.

New glass formulation was found in the SciGlass® database with criteria of CTE between 10.5 and 11 and glass transition temperatures near 600° C and it is referred to as KMBY. The glass compositional ranges are reported in table 1.

The sealants was produced as glass by melting the appropriate oxides and carbonates raw materials in different proportions (as reported in table 1) and by heating at 1500°C for 1 hour in a platinum-rhodium crucible; the melt was cast on a brass plate and the transparent glass was ground for differential thermal analysis (DTA) (Netzsch, Eos, Germany) and hot stage microscopy (HSM) (Expert System solutions, Italy) experiments.

The glass was powdered and sieved into 3 different size ranges: <38 μm, 38÷75 μm and > 75 μm. The characteristic temperatures of the sealant compositions and the shrinkage behaviour vs temperature were measured by DTA (3 samples were used to determine the glass transition temperature ; T_g was taken at the onset, obtained by the intersection of the two tangents at the start of the endotherm) and heating stage microscopy. The thermal behaviour of the glass powder as a function of the particle size by DTA was analysed only for KMBY. DTA scans were recorded from room temperature to 1200°C with heating rates of 5, 10, 20°C/min respectively. Coefficients of thermal expansion (CTE) were measured on both glass and glass-ceramic samples (5×5×4 mm^3) with heating rate of 5°C/min; glass ceramic samples were prepared by uniaxially pressing glass powders (<38 μm) and subsequent heat treatment at 850°C, 30 minutes in Ar atmosphere. Three samples were used for determination of the mean CTE value and the error was ± 0.16.

Characteristic shapes corresponding to first shrinkage (T_{FS}), maximum shrinkage (T_{MS}), deformation (T_D), sphere (T_B), half-ball (T_{HB}) and flow (T_F) points were extracted from HSM experiments at 5 and 20°C/min respectively.

Prior to the joining process Crofer22APU samples were coated by a $Mn_{1.5}Co_{1.5}O_4$ protective layer; the $Mn_{1.5}Co_{1.5}O_4$ was deposited on Crofer22APU by thermal co-evaporation technique using a Theva GmbH evaporation system. The used process is described more in detail elsewhere [18]. Briefly, Mn (99.8% purity) and Co (99.9%), from Chempur GmbH, were used as raw materials and put them in two separate boat crucibles and positioned in the evaporation chamber. The deposition experiments were performed by resistively heating the respective boat crucibles with the applied power. The deposition pressure of about 2×10^{-5} mbar was maintained by two turbo molecular vacuum units during the 30 min of evaporation. The substrate holder was heated and retained at temperature 600 °C by resistive heaters located above it. After thermal co-evaporation, the samples were annealed *in-situ* at 800 °C for 30min in 1 atm of O_2 gas in order to form the Mn–Co spinel phase coating. The thickness of the $Mn_{1.5}Co_{1.5}O_4$ layer was found to be around 1 µm with high degree of reproducibility. Details of experiments are reported in a previous paper [18].

The joined samples were prepared by depositing a slurry of powder of the glass (<38 µm with 40% solid content dispersed in ethanol) onto a plate of the yttria-stabilised zirconia (YSZ) surface of the anode-supported electrolyte. A plate of the Crofer22APU was then placed on top so that the slurry was sandwiched between the anode-supported electrolyte and the interconnect materials.

The joining thermal treatment was carried out by heating from room temperature to 850°C at a heating rate of 5 °C/min and a dwelling time of 30 minutes. The cooling rate was 5 °C/min. Dilatometric measurements were conducted both on the glass and the glass-ceramic bulk samples; the glass sample (as obtained by casting the glass on the brass plate) was machined to a cylinder (5 mm height), while the glass-ceramic cylinder was obtained by uniaxially pressing of glass

powders (<38 μm) and subsequent heat treatment at 850°C, 30 min (ethanol was used as a binder in preparing the sintered samples) . For comparison purposes, also a second glass-ceramic sample was prepared with a holding time of 120 min at 850°C.

Glass powders and glass-ceramic powders were subjected to X-ray powder diffraction (XRD, Bruker AXS D8 Advance, Karlsruhe, Germany), employing CuKα radiation (0.15418 nm); the analysis was repeated, for the glass-ceramic powders, after mixing with corundum (crystalline alumina) powders, operating as internal standard. The diffraction patterns were analysed by means of "Match!" software (Crystal Impact GbR, Bonn, Germany), supported by data from PDF-4 database (International Centre for Diffraction Data – ICDD, Newtown Square, PA). Mineralogical quantitative phase analysis (QPA), based on the Rietveld method [21], was performed using TOPAS software (Bruker AXS, version 4.1, Karlsruhe, Germany). The contents of crystalline and amorphous phases were determined using the combined Rietveld–RIR method [22, 23].

Thermal tests were performed in a muffle furnace in static air from room temperature to 800°C at a rate of 5°C/min and dwelling for 100 hours followed by cooling slowly in the furnace down to room temperature then repeating the same cycle until 500 hours.

Cross-sections of joined samples were characterized by scanning electron microscopy (SEM), JEOL 5700) after polishing; Au was sputtered on the samples submitted to SEM observation, in order to make samples conductive for electron microscopy. Energy dispersive X-ray spectroscopy (EDX) microanalysis was carried out in order to detect any elemental diffusion into or away from the sealant before and after thermal cycling and to examine for any chemical interactions between the $Mn_{1.5}Co_{1.5}O_4$ coated Crofer22APU and the anode-supported-electrolyte with the glass-ceramic sealant.

3. Results and discussion

Glass-ceramic materials are usually produced through the sintering of glass powders. In this case, sintering and crystallization processes can interact, thus affecting the final density of glass-ceramics materials. The densification of a glass powder compact is obtained through viscous flow at temperatures higher than the glass softening point. The correct order of events in a glass-powder sintering process is a critical issue which enables the formation of a dense glass-ceramic material. Particular focus must be given to the sintering- crystallization equilibrium: when a powder compact of glass particles is sintered, the maximum shrinkage is reached when larger pores have disappeared due to the viscous flow. With increasing sintering time three different conditions can occur, depending on surface crystallization vs viscous flow sintering "competition":

- pure viscous sintering of glass occurs if excessive sintering takes place at the expense of poor surface crystallization.
- excessive surface crystallization occurs before the end of the sintering stage (or maximum shrinkage), as a consequence, the viscous flow is limited by crystallization; the final result is a porous glass-ceramic materials.
- optimum conditions are obtained when the sintering process is completed before surface crystallization begins. In these conditions, dense glass-ceramic materials are obtained.

Figure 1 shows the DTA curves (heating rate 20 °C/min) of glass powders sieved at 3 different particle size ranges and of the bulk glass. The T_g is found to be around 600 °C and one exothermic peak (corresponding to the crystallisation of the glass) can be detected at higher temperatures. The crystallization peak is considerably affected by the particle size; in fact the peak shifted to lower temperatures with decreasing particle size, suggesting a possible effect associated with the surface crystallization of the glass [24]. A decrease in the crystallization peak height with increasing particle size can be also observed; this behaviour also suggests that the crystalline phase formation starts mainly on the surface of the glass particles.

The sintering behaviour of the KMBY glass was examined by hot-stage microscopy (HSM), along with microstructural observations at characteristic points as reported in figure 2. It can be observed that maximum shrinkage is reached at around 850°C (heating rate: 5°C/min); on the basis of the HSM observations, 850°C was chosen as the joining temperature, since it is expected that complete densification should be obtained at this point. Plots of shrinkage against temperature yielded characteristic temperatures as summarized below:

1. First shrinkage or sintering (T_{FS}): temperature at which the linear shrinkage of the glass starts ($\log \eta = 9.1 \pm 0.1$); this step starts above the glass Tg. Maximum shrinkage (T_{MS}): temperature of maximum shrinkage before the glass starts to soften ($\log \eta = 7.8 \pm 0.1$).
2. Softening/Deformation point (T_D): temperature at which the first signs of softening are observed, highlighted by the rounding of the corners of the sample ($\log \eta = 6.3 \pm 0.1$).
3. Sphere temperature (T_B): temperature at which the height of the sample is equal to the width of the base according to the standards or at which the diameter is the double of the ray of an hypothetical circumference.
4. Half ball point (T_{HB}): temperature at which the height of the sample is half the width of the base ($\log \eta = 4.1 \pm 0.1$).
5. T flow (T_F): temperature at which the height of the sample shrinks to under a third of the base and the sample is completely melt ($\log \eta = 3.4 \pm 0.1$).

From these points, it was possible to plot a viscosity–temperature curve [25] (figure 3), and a value of viscosity around 10^5 Pa s was obtained at a temperature of 850°C; HSM data (temperature values) are obtained with an error of ± 10°C; log η (Poise) values are obtained with an error of ± 0.1. This value is appropriate to allow a good bonding with the Crofer22APU substrate and it was in good agreement with the value suggested by other authors et al. [26] as the ideal sealing viscosity average value in a SOFC planar geometry.

Furthermore, comparing the HSM data with DTA analysis (Figure 1 and 2, respectively) it can be concluded that the process of sintering and crystallization are independent of each other since T_x (the onset of crystallization) is detected after the T_{MS}. Since the sintering process is completed before surface crystallization begins, the formation of a dense glass-ceramic sealant material is expected.

Dilatometer curves of both the glass and of the glass-ceramic sealant (after a heat treatment at 850°C, 30 min, Ar) are reported in figure 4; coefficient of thermal expansion (CTE) values of 8.5 x 10^{-6} and 10.9 x 10^{-6} for the glass and for the glass-ceramic were obtained respectively, thus providing an excellent thermo-mechanical compatibility of the glass-ceramic sealant with both the Crofer22APU and the anode-supported-electrolyte. Moreover, after the crystallization heat-treatment (850°C for 30 min) a residual glassy phase with Ts (dilatometric softening point) of 773°C can still be detected. Rigid glass seals are prone to cracking when exposed to the SOFC device operating conditions as a consequence of the thermal cycles. In order to overcome this problem, the design of self-healing glass compositions can be a possible and viable solution. In the system which was studied here, the residual glassy phase could heal possible cracks formed during thermal cycling by viscous flow sealing at temperatures in excess of 770°C which is very close to the SOFC operating temperature. In case of any crack formation, the proposed sealant will therefore have the potential to restore its hermeticity upon being reheated to the solid oxide fuel cell stack operating temperature. Furthermore, it is also worthy to note that crystalline phases can enhance the viscosity of the system, thus providing improved thermo mechanical stability of the joining area.

An SEM image of the $Mn_{1.5}Co_{1.5}O_4$ coated Crofer22APU-glass-ceramic sealant-anode supported electrolyte cross section is presented in figure 5.

The joint region has an average thickness of 300 µm. Examination around the joined area shows an homogeneous and very dense glass-ceramic sealant, as a result of an excellent sintering and densification behaviour, indicating that it will provide high gas tightness and a hermetic structure.

A very good adhesion between the glass–ceramic and both Crofer22 APU and YSZ can also be observed.

EDS point analyses performed on different areas labelled as A and B in figure 6 suggested the presence of diopside crystals together with a significant amount of a residual glassy phase. This was confirmed by results of XRD analysis of the glass-ceramic sample (reported in figure 7); diopside ($Ca_{0.89}Mg_{1.11}Si_2O_6$, PDF#87-0689) and potassium-containing nepheline ($Na_3K(Al_{0.44}Si_{0.56})_8O_{16}$, PDF#76-2469) were detected together with minor traces of akermanite ($Ca_2MgSi_2O_7$, PDF#76-0841) and a substantial amount of a residual amorphous phase (testified by the significant "amorphous halo" in the pattern).

The refinement of the pattern of the sample constituted by glass-ceramic powders mixed with corundum powders, by means of the Rietveld's method, allowed for the quantification of the crystal phases. More precisely, since the TOPAS software could provide only the relative contents of crystal phases, the absolute quantities of crystal phases and residual glass phase were computed on the basis of the content of corundum standard (known a priori). The quantities of the different phases are shown in Tab. 2.

Diopside is the dominant crystal phase, while nepheline is quite limited, in the sample treated at 850°C for 30 min. The amount of nepheline was found to increase for a longer treatment (120 min), which also determined the practical dissolution of akermanite.

An elemental line scan using SEM-EDX analysis at the $Mn_{1.5}Co_{1.5}O_4$ coated Crofer22APU-glass-ceramic sealant interface is presented in Fig 8. It shows that there was no diffusion of either chromium or manganese from the Crofer22APU; in addition, there was no manganese diffusion from the $Mn_{1.5}Co_{1.5}O_4$ layer into the glass-ceramic. A small amount of Cr diffusion can be observed at the interface between the Crofer22APU and the $Mn_{1.5}Co_{1.5}O_4$ coating; this is probably due to heat treatment in air at 800°C for 2 hours; this is necessary for densification of the $Mn_{1.5}Co_{1.5}O_4$ coating after co-evaporation deposition.

SEM examination of the samples for both thermal cycles after 500 hrs showed that the $Mn_{1.5}Co_{1.5}O_4$- coated Crofer22APU and the glass-ceramic sealant interface remained adhered together, and consequently both interfaces (Crofer22APU/ $Mn_{1.5}Co_{1.5}O_4$ and $Mn_{1.5}Co_{1.5}O_4$ /glass-ceramic) were still sound and free of cracks. a well-bonded interface is still present, without evidence of coating spallation despite of the thermal cycles.

For a better understanding of the elemental distribution across the interface and in order to study the Cr behaviour with respect to $Mn_{1.5}Co_{1.5}O_4$ layer protection effectiveness, an EDS elemental map is shown in figure 9; it can be observed that the $Mn_{1.5}Co_{1.5}O_4$ was very effective in preventing Cr diffusion into the glass-ceramic sealant. In fact Cr was found to be confined just beneath the $Mn_{1.5}Co_{1.5}O_4$ layer, a behaviour similar to the as joined condition, Furthermore the microstructure and compositional analysis clearly indicated that also Mn and Fe did not diffuse into the glass-ceramic sealant. $Mn_{1.5}Co_{1.5}O_4$ protective layer was also useful in order to avoid the possible reaction between alkali (Na_20 and K_20 with Cr).

An SEM micrograph showing the glass-ceramic/YSZ interface after the thermal cycling is reported in Fig. 10 ; this revealed the strong adherence of the glass-ceramic sealant to the YSZ and showed that the interface was free from cracks and pores. The YSZ electrolyte was not cracked and was still adhered to the anode functional layer. Furthermore, no elemental diffusion was detected into the sealant (EDS not reported here), and consequently no new phases were formed at the YSZ/glass-ceramic sealant interface. EDS points analyses were conducted in different areas labelled as 1, 2 and 3 respectively are reported in Table 3. This observation confirmed the presence of the original diopside and nepheline crystalline phases together with a significant amount of residual glassy phase, thus demonstrating the stability of the glass-ceramic sealant after 500 hrs of thermal cycling in air.

The paper that is presented here showed the stability with YSZ electrolyte and a $Mn_{1.5}Co_{1.5}0_4$ based coated interconnect; this glass-ceramic can only be considered as sealant between the

electrolyte and the metal; in order to qualify this glass-ceramic as sealant between two interconnect plates, electrical properties will be measured in order to complete the characterization and the validation of the proposed sealant; a future work will be presented concerning the behaviour of the sealant in a real SOFC short stack, thus showing no cathode poisoning due to volatilized species formation.

The long term stability of the glass-ceramic sealant is also an important issue. The percentage of the glassy phase evaluation after a long term test will be also shown in a follow up paper.

Conclusions

A novel glass-ceramic to be used as sealant for planar solid oxide fuel cells and its compatibility with $Mn_{1.5}Co_{1.5}O_4$ coated Crofer22APU have been presented and discussed. The sealant showed homogeneous and very dense microstructure, as a result of an excellent sintering and densification behaviour. XRD analysis of the glass-ceramic and Rietveld refinement showed diposide ($Ca_{0.89}Mg_{1.11}Si_2O_6$) as the main crystalline phase and substantial amount of a residual amorphous phase. The interfacial compatibility with $Mn_{1.5}Co_{1.5}O_4$ coated Crofer22APU and YSZ (anode supported) was found to be very good, also after 500 hours of thermal cycling (RT-800) in air atmosphere, since no cracks formation, interactions, or failure were observed. Finally, The $Mn_{1.5}Co_{1.5}O_4$ coating was effective in preventing diffusion of Cr and Mn and adverse reactions at the Crofer22APU/ $Mn_{1.5}Co_{1.5}O_4$ /sealant interface.

Acknowledgments

The research leading to these results has received funding from the European Union's Seventh Framework Programme managed by REA-Research Executive Agency

http://ec.europa.eu/research/rea and it participates in a Marie Curie Action (GlaCERCo GA 264526). KMM-VIN mobility grant for Dr. Federico Smeacetto is also acknowledged.

References

[1] B. C. H. Steele and A. Heinzel," Materials for Fuel Cell Technology*", Nature,* **414**, 345–352 (2001).

[2] R. N. Singh, "Sealing Technology for SOFCs", *Int. J. Appl. Ceram. Technol.*, **4** [2] 134–44 (2007).

[3] J. Schilm, A. Rost, A. Poenicke, M. Kusnezoff, and A. Michaelis, "Ceramic Integration Technologies for Solid Oxide Fuel Cells", *Int. J. Appl. Ceram. Technol.*, **9** [4] 688–699 (2012).

[4] I. W. Donald, P. M. Mallinson, B. L. Metcalfe, L. A. Gerrard, and J. A. Fernie, "Recent developments in the preparation, characterization and applications of glass- and glass–ceramic-to-metal seals and coatings", *J. Mater. Sci.*, **46** [7] 1975–2000 (2011).

[5] R. Jordan, ''Is the Future of SOFCs Sealed in Glass?,'' *Am. Ceram. Soc. Bull.*, **87** [1] 26–29 (2008).

[6] D. Coillot, F. O Mear, H. Nonnet, and L. Montagne, "New viscous sealing glasses for electrochemical cells", *Int. J. of Hyd. Energy*, **37** [11] 9351-9358 (2012).

[7] Y. S. Chou, J. W. Stevenson, and K. D. Meinhardt, "Electrical Stability of a Novel Refractory Sealing Glass in a Dual Environment for Solid Oxide Fuel Cell Applications", *J. Am. Ceram. Soc.*, **93** [3] 618–623 (2010).

[8] F. Smeacetto, M . Salvo, P. Leone, M. Santarelli, and M. Ferraris," Performance and testing of joined Crofer22APU-glass-ceramic sealant-anode supported cell in SOFC relevant conditions", *Mater. Lett.*, **65** [6] 1048–52 (2011).

[9] C. Thieme and C. Rüssel, "Cobalt containing crystallizing glass seals for solid oxide fuel cells - A new strategy for strong adherence to metals and high thermal expansion", *J. Power Sources*, **258** 182-188 (2014).

[10] Y. S. Chou, J. W. Stevenson, and J. P. Choi, "Long-term evaluation of solid oxide fuel cell candidate materials in a 3-cell generic short stack fixture, part I: Test fixture, sealing, and electrochemical performance", *J. Power Sources*, **255** 1-8 (2014).

[11] D. U. Tulyaganov, A. A. Reddy, V. V. Kharton, and J. M. F. Ferreira, Aluminosilicate-based sealants for SOFCs and other electrochemical applications - A brief review, *J. Power Sources* **242** [15] 486-502 (2013).

[12] A. Shyam, R. Trejo, D. McClurg, A. Ladouceur, M. Kirkham, X. Song, J. Howe , and E. Lara-Curzio, "Microstructural evolution in two alkali multicomponent silicate glasses as a result of long-term exposure to solid oxide fuel cell environments", *J. Mater .Sci* ., **48** 5880–5898 (2013).

[13] H. Abdoli, P. Alizadeh, and K. Agersted, "Fabrication and sealing performance of rare-earth containing glass–ceramic seals for intermediate temperature solid oxide fuel cell applications", *Ceram. Int.*, **40** [5] 7545–7554 (2014).

[14] F. Smeacetto, A. Chrysanthou, M. Salvo, T. Moskalewicz, F. D. D'Herin Bytner, L. C. Ajitdoss, and M. Ferraris," Thermal cycling and ageing of a glass-ceramic sealant for planar SOFCs". *Int. J. Hyd. En*, **36** [18] 11895-11903 (2011).

[15] Y Liu, J. W. Fergus, and C. Dela Cruz, "Electrical Properties, Cation Distributions, and Thermal Expansion of Manganese Cobalt Chromite Spinel Oxides", *J. Am. Ceram. Soc.*, **96** [6] 1841–1846 (2013).

[16] Y. Zhang, A. Javed, M. Zhou, S. Liang, and P. Xiao, "Fabrication of Mn–Co Spinel Coatings on Crofer 22 APU Stainless Steel by Electrophoretic Deposition for Interconnect Applications in Solid Oxide Fuel Cells", *Int. J. Appl. Ceram. Technol.*, **11** [2] 332–341 (2014).

[17] J. P. Choi, K. S. Weil, Y. S. Chou, J. W. Stevenson, and Z. G. Yang, "Development of MnCoO coating with new aluminizing process for planar SOFC stacks", *Int. J. Hydrogen Energ.*, **36** 4549-4556 (2011).

[18] L.C. Ajitdoss, F. Smeacetto, M. Bindi, D. Beretta, M Salvo, and M. Ferraris, "$Mn_{1.5}Co_{1.5}O_4$ protective coating on Crofer22APU produced by thermal co-evaporation for SOFCs", *Mater. Lett.* , **95** 82–85 (2013).

[19] Y. S. Chou, J. W. Stevenson, and J. P. Choi, "Evaluation of a Single Cell and Candidate Materials with High Water Content Hydrogen in a Generic Solid Oxide Fuel Cell Stack Test Fixture, Part II: Materials and Interface Characterization", *Int. J. Appl. Ceram. Technol.*, **10** [1] 97–106 (2013).

[20] M.K. Mahapatra and K. Lu, "Seal glass compatibility with bare and (Mn,Co)3O4 coated Crofer 22 APU alloy in different atmospheres", *J. Power Sources,* **196** 700–708 (2011).

[21] H.M. Rietveld," A profile refinement method for nuclear and magnetic structures", *J. Appl. Crystallogr.*, **2** 65-71(1969)

[22] A. F. Gualtieri, "Accuracy of XRPD QPA using the combined Rietveld–RIR method", *J. Appl. Crystallogr.*, **33** 267–278 (2000).

[23] W. A. Dollase, " Correction of intensities for preferred orientation in powder diffractometry: application of the March model", *J. Appl. Crystallogr.*, **19** 267–72 (1986).

[24] A. A. Francis, R. D. Rawlings, R. Sweeney, and A. R. Boccaccini, "Crystallization kinetic of glass particles prepared from a mixture of coal ash and soda-lime cullet glass", *J. Non Cryst. Solids*, **333** 187–193 (2004).

[25] M. J. Pascual, A. Durán, and M. O. Prado, "A new method for determining fixed viscosity points of glasses", *Phys. Chem. Glasses.*, **46** [5] 512–520 (2005).

[26] M.O. Naylor, T. Jin, J.E. Shelby, and S.T. Misture, "Galliosilicate glasses for viscous sealants in solid oxide fuel cell stacks: Part I: Compositional design", *Int. J. Hyd. En*, **38** [36] 16300-16307 (2013).

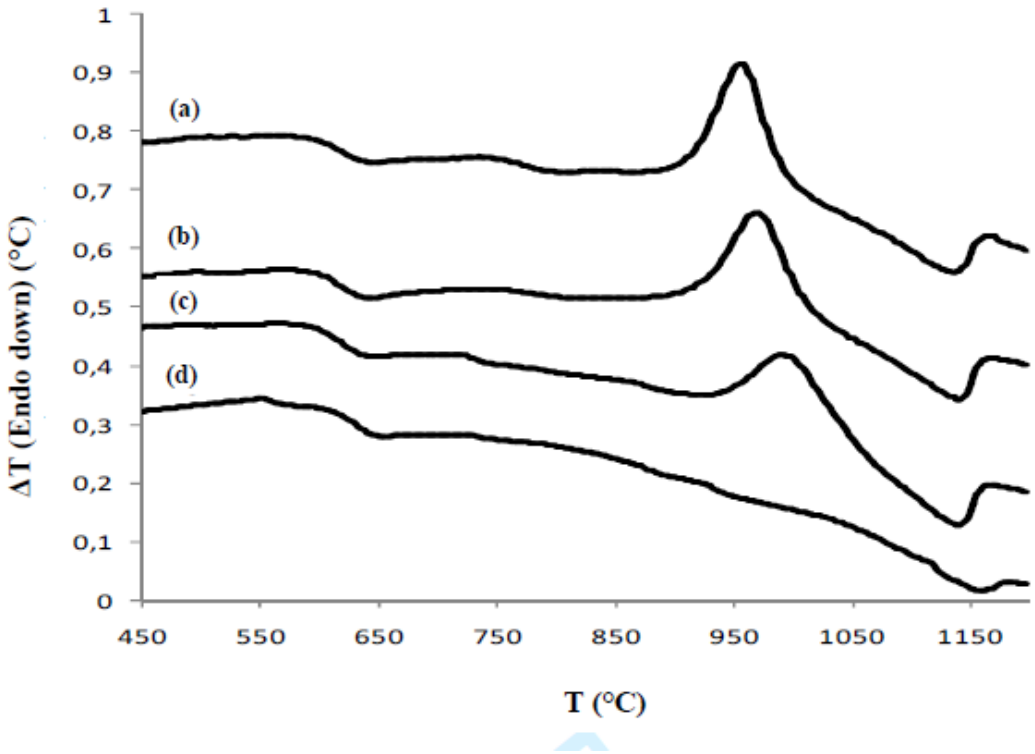

Figure 1 DTA curves (heating rate 20 °C/min) of glass powders sieved at 4 different mean particle size ranges and of the bulk glass. (a) < 38 µm, (b)38 < µm < 75, (c) > 75 µm, (d) bulk glass.

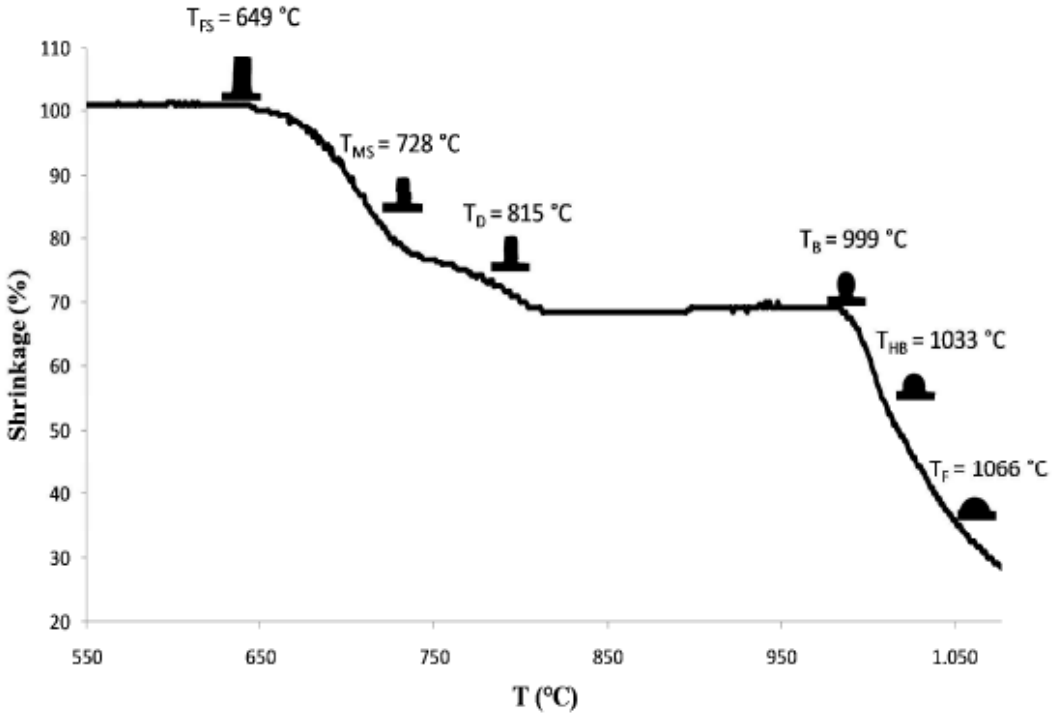

Figure 2 Heating stage microscopy, together with pellet images at characteristic viscosity points

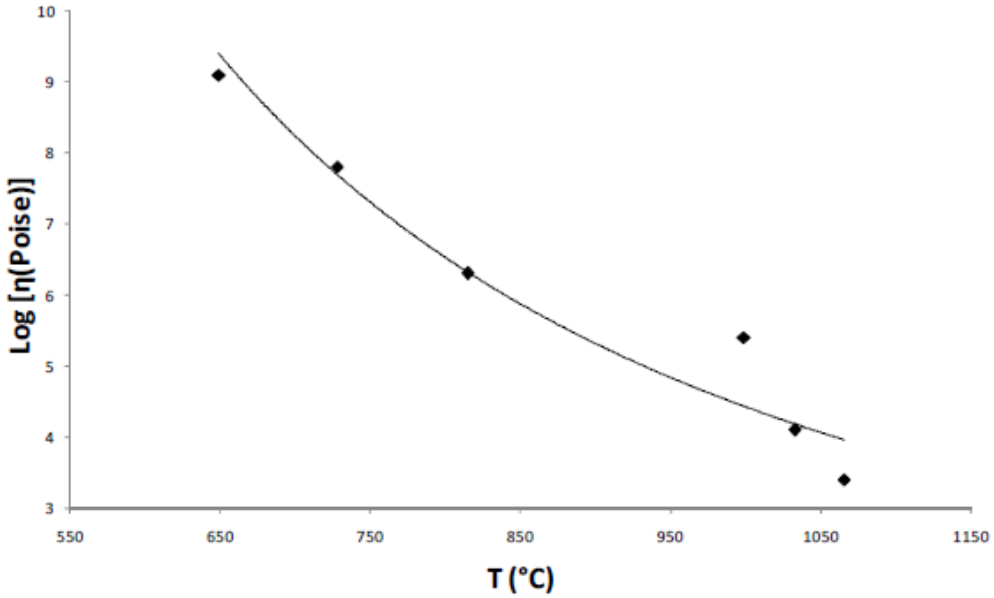

Figure 3 Viscosity–temperature curve for KMBY glass-based sealant

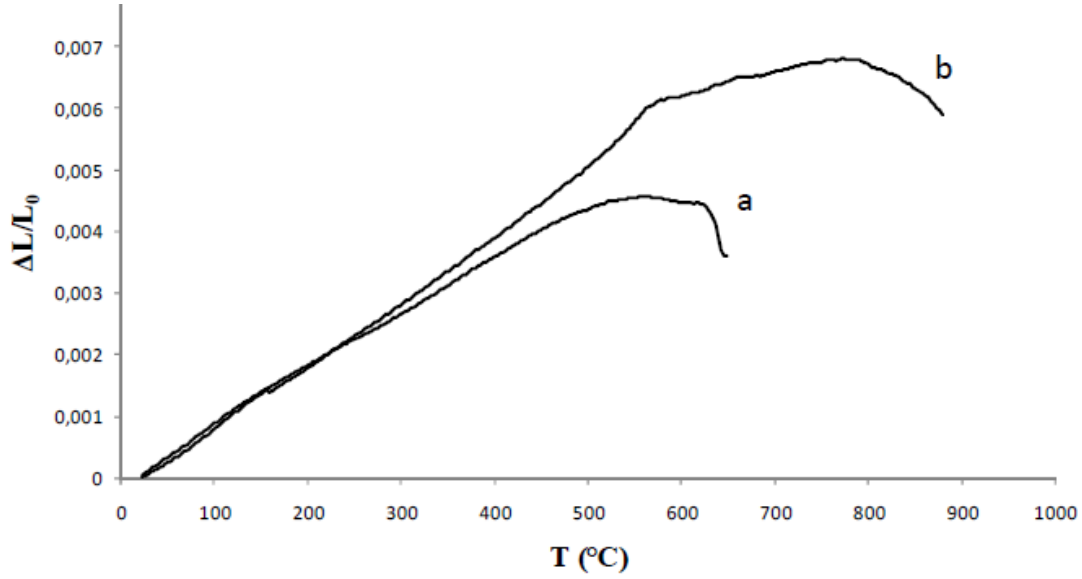

Figure 4 Dilatometer curves of both the glass (a) and of the glass-ceramic sealant (b)

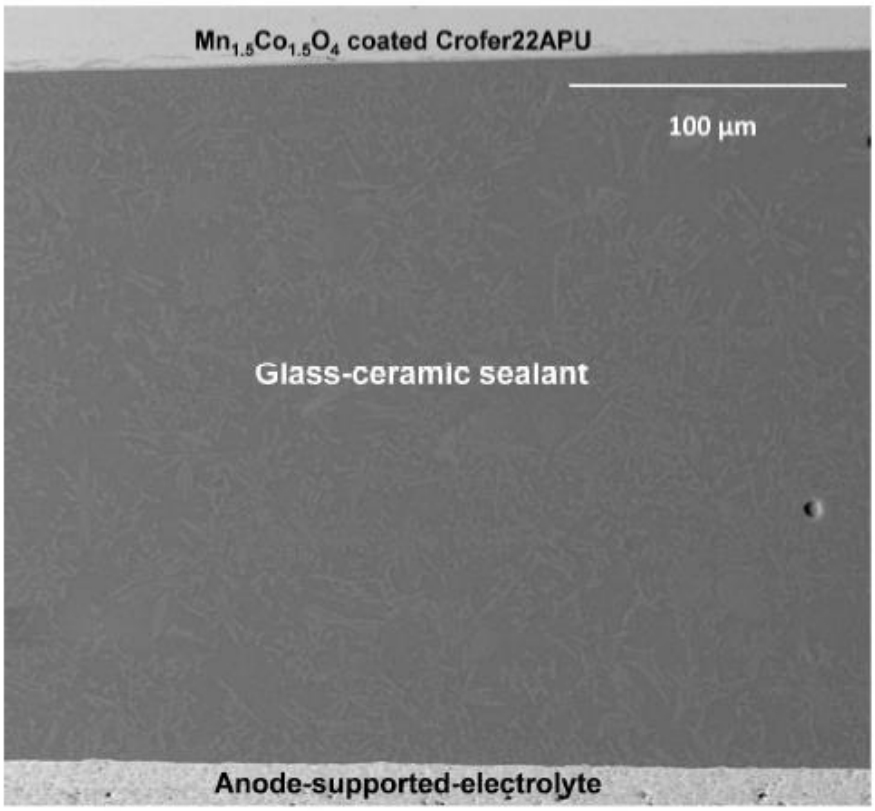

Figure 5 SEM image of the Mn1.5Co1.5O4 coated Crofer22APU-glass-ceramic sealant-anode supported electrolyte cross section after joining heat treatment at 850°C, 30 minutes.
387x361mm (300 x 300 DPI)

Figure 5 SEM image of the $Mn_{1.5}Co_{1.5}O_4$ coated Crofer22APU-glass-ceramic sealant-anode supported electrolyte cross section after joining heat treatment at 850°C, 30 minutes.

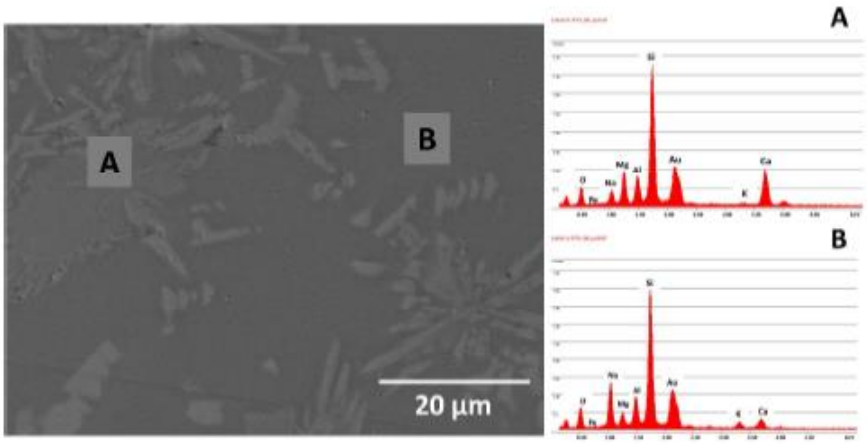

Figure 6 EDS point analyses performed on different areas labelled as A and B
493x259mm (300 x 300 DPI)

Figure 6 EDS point analyses performed on different areas labelled as A and B

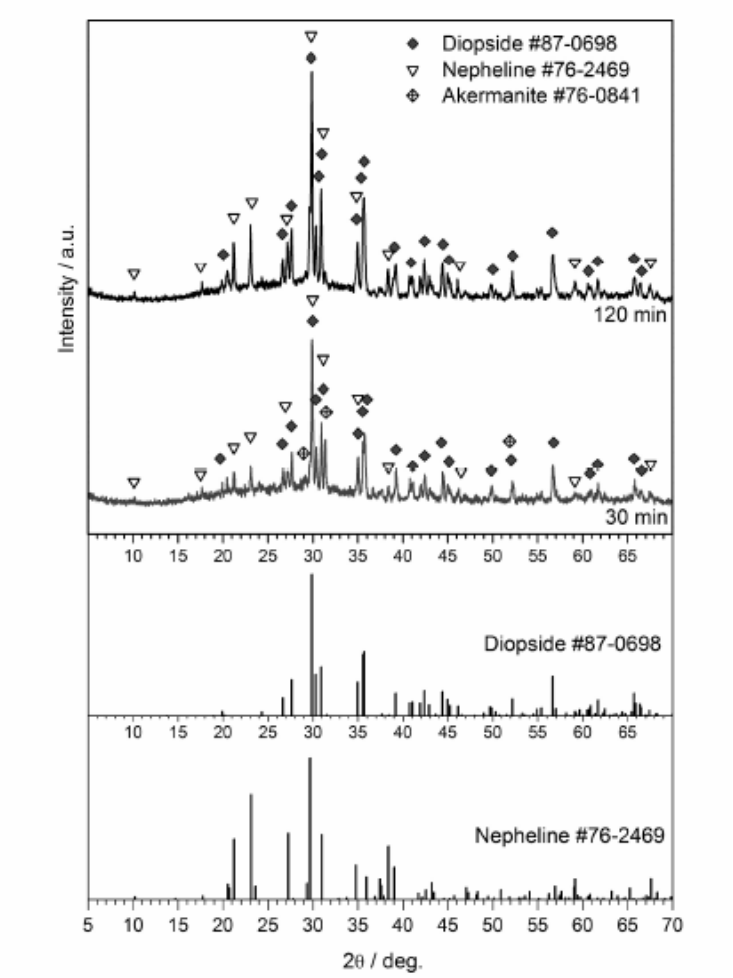

Figure 7 XRD pattern on glass-ceramic after 850°C, after heat treatment of 30 and 120 min
209x293mm (300 x 300 DPI)

Figure 7 XRD pattern on glass-ceramic after 850°C, after heat treatment of 30 and 120 min

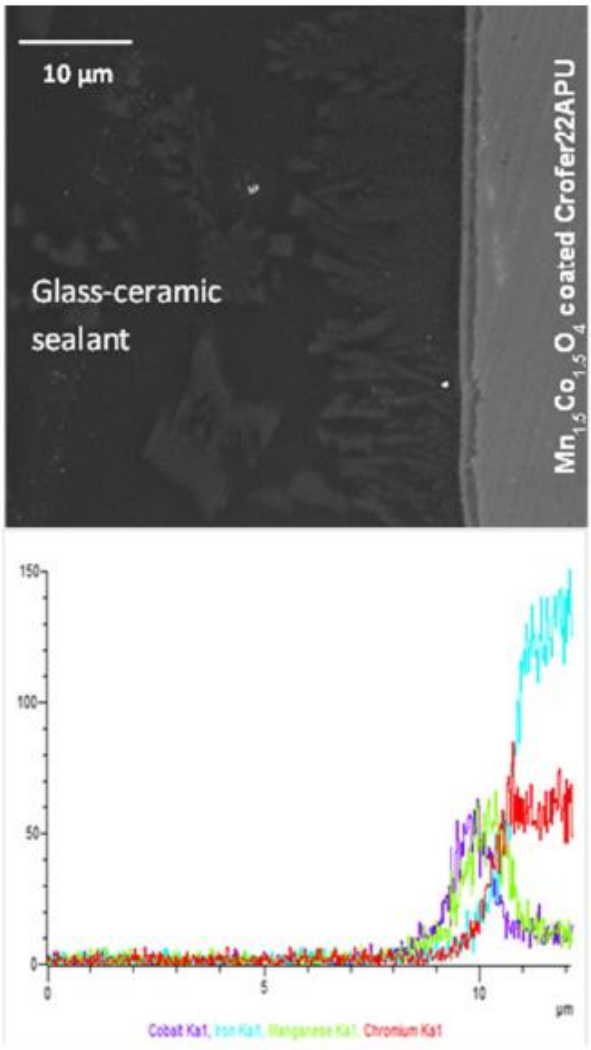

Figure 8 Elemental line scan using SEM-EDX analysis at the Mn1.5Co1.5O4 coated Crofer22APU-glass-ceramic sealant interface after 850°C, 30 min
171x305mm (300 x 300 DPI)

Figure 8 Elemental line scan using SEM-EDX analysis at the $Mn_{1.5}Co_{1.5}O_4$ coated Crofer22APU-glass-ceramic sealant interface after 850°C, 30 min

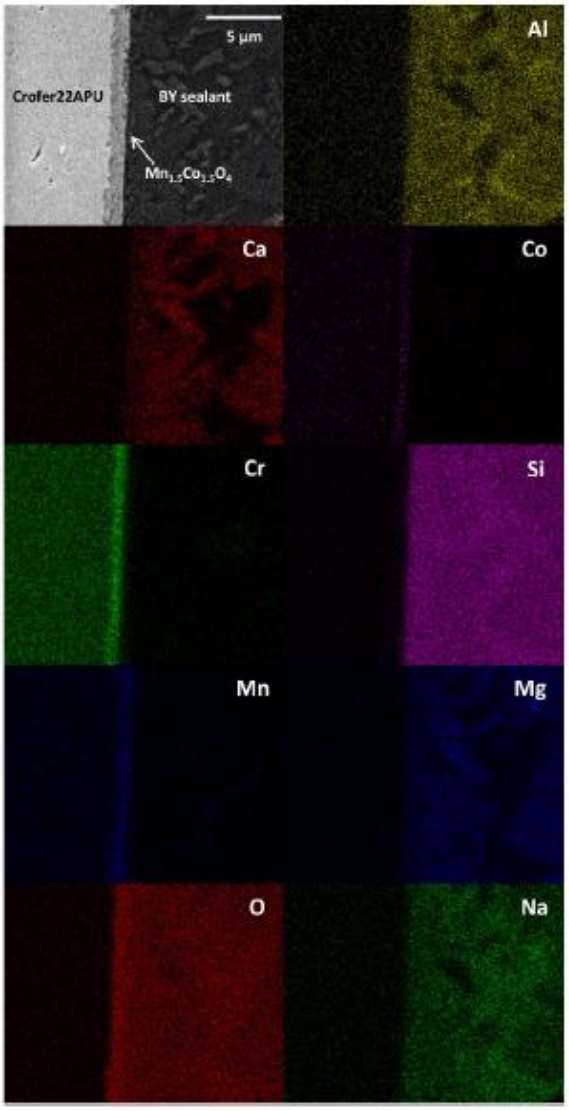

Figure 9 Mn1.5Co1.5O4 coated Crofer22APU/glass-ceramic sealant interface after 500 hrs of thermal cycling
262x508mm (300 x 300 DPI)

Figure 9 $Mn_{1.5}Co_{1.5}O_4$ coated Crofer22APU/glass-ceramic sealant interface after 500 hrs of thermal cycling

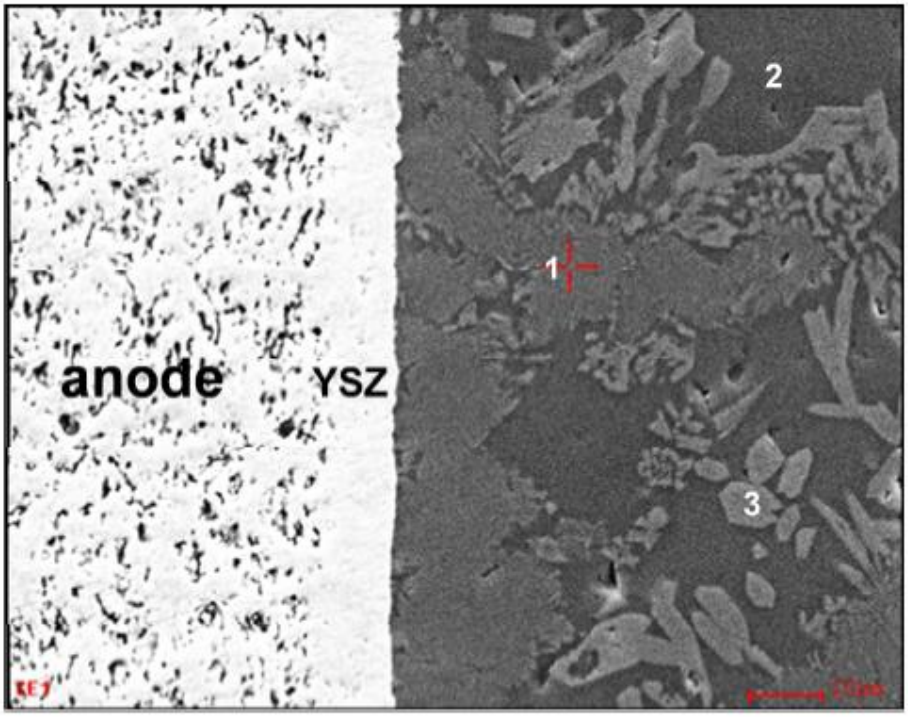

Figure 10 SEM micrograph showing the glass-ceramic/YSZ interface after 500 hrs of thermal cycling
227x178mm (300 x 300 DPI)

Figure 10 SEM micrograph showing the glass-ceramic/YSZ interface after 500 hrs of thermal cycling

Table 1 Glass sealant (KMBY) compositional range (wt%)

	SiO_2	Al_2O_3	CaO	Na_2O	others
KMBY glass (wt%)	54	11	9	14	K_2O, MgO, B_2O_3 and Y_2O_3

Table 2 Results from quantitative X-ray diffraction analysis

Phase	Content (wt%)	
	After 850 °C, 30 min	After 850 °C, 120 min
Amorphous phase	62.4	54.3
Diopside	26.8	31.6
Nepheline	6.8	13.2
Akermanite	4.0	0.9

Table 3 EDS points analyses conducted in different areas labelled as 1, 2 and 3 for glass-ceramic/YSZ interface after 500 hrs of thermal cycling

Element At%	*Point 1*	*Point 2*	*Point 3*
O	51.23	52.00	52.53
Na	05.95	09.94	
Mg	06.96	03.27	11.15
Al	06.40	05.72	00.51
Si	23.73	28.43	25.34
Ca	05.73	00.63	10.46